ELSEVIER

Journal of Organometallic Chemistry 558 (1998) 197–207

Journal of Organo metallic Chemistry

Coupling of 1,3-diynes on a triruthenium cluster: reactions of $Ru_3(\mu_3\text{-}PhC_2C{\equiv}CPh)(\mu\text{-dppm})(CO)_8$ with $SiMe_3C{\equiv}CC{\equiv}CSiMe_3$

Michael I. Bruce [a,*], Brian W. Skelton [b], Allan H. White [b], Natasha N. Zaitseva [a]

[a] *Department of Chemistry, University of Adelaide, Adelaide, SA 5005, Australia*
[b] *Department of Chemistry, University of Western Australia, Nedlands, WA 6907, Australia*

Received 20 November 1997

Abstract

Reactions between $Ru_3(\mu_3\text{-}PhC_2C{\equiv}CPh)(\mu\text{-dppm})(CO)_8$ (**1**) and $SiMe_3C{\equiv}CC{\equiv}CSiMe_3$ have given the complexes $Ru_2(\mu\text{-dppm})\{\mu\text{-}C(C{\equiv}CPh){=}CPhC(SiMe_3){=}C(C{\equiv}CSiMe_3)\}(CO)_4$ (**3**), containing the two diynes coupled in head-to-head fashion, $Ru_3\{\mu_3C(SiMe_3){=}C(C{\equiv}CSiMe_3)C({=}CPh)C({=}CPh)C(O)\}(\mu\text{-dppm})(CO)_7$ (**4**), containing a metalla–indenone ligand formed by coupling of the two diynes with CO, and $Ru_4(\mu_4\text{-}PhC_2C{\equiv}CPh)(\mu_4\text{-}SiMe_3C_2C{\equiv}CSiMe_3)(\mu\text{-dppm})(\mu\text{-}CO)(CO)_8$ (**6**), in which the two diynes are on opposite sides of a puckered Ru_4 rhomboid. Also formed were thermolysis products of **1**, $Ru_3\{\mu_3\text{-}CPhCHCC(C_6H_4)\}(\mu\text{-dppm})(CO)_8$ (**5**) (previously described) and $Ru_4(\mu_4\text{-}PhC_2C{\equiv}CPh)(\mu\text{-dppm})(CO)_{10}$ (**7**), the dppm-substitution product of $Ru_4(\mu_4\text{-}PhC_2C{=}CPh)(CO)_{12}$. The X-ray determined structures of **3**, **6** and **7** are reported. © 1998 Elsevier Science S.A. All rights reserved.

Keywords: Ruthenium clusters; Coupling of 1,3-diynes

---

1. Introduction

Reactions of alkynes with the cluster carbonyls of ruthenium and osmium continue to yield complexes with unusual structures [1]. Studies of the reactions of 1,3-diynes have shown that while complexes of similar types to those formed with monoynes can be obtained, in which the second alkynyl group acts as a simple substituent [2], other reactions can also be observed. These include cleavage of the diyne into two alkynyl fragments, as found in the thermolysis of $Os_3(\mu_3\text{-}PhC_2C{\equiv}CPh)(CO)_{10}$, which gave a cluster containing μ_2- and μ_3-C_2R ligands [3]. A similar observation was made with the synthesis of the mixed-metal cluster $Co_2Ru_3(\mu_4\text{-}C_2Ph)(\mu_3\text{-}C_2Ph)(\mu\text{-dppm})(CO)_{11}$ [4]. Larger clusters can interact with both C≡C triple bonds, leading to extended coordination of the diyne over the cluster. Subsequent reactions have given a range of unusual ligands. For example, coordination of $PhC{\equiv}CC{\equiv}CPh$ to $Ru_4(\mu_3\text{-}PPh)(CO)_{13}$ gave $Ru_4\{\mu_4\text{-}PPhC(C{\equiv}CPh)CPh\}(CO)_{12}$ which decarbonylated on heating to $Ru_4(\mu_4PPh)(\mu_4\text{-}PhC_2C{\equiv}CPh)(CO)_{10}$. Addition of $PhC{\equiv}CC{\equiv}CPh$ then gave Ru4(μ_4-PPh)$\{\mu_4C_4Ph_2(C{\equiv}CPh)CCCPhC(C{\equiv}CPh)CPh\}(CO)_8$ [5]. Related reactions with $Ru_4(\mu\text{-}H)_2(\mu_3\text{-}PPh)(CO)_{12}$ have also been described [6].

Continuing our own studies on the reactions between the triruthenium cluster carbonyls $Ru_3(CO)_{12}$ and $Ru_3(\mu\text{-dppm})(CO)_{10}$ and 1,4-diphenylbuta-1,3-diyne [2,7], we have examined the reactions of the complex $Ru_3(\mu_3\text{-}PhC_2C{\equiv}CPh)(\mu\text{-dppm})(CO)_8$ (**1**) with an excess of $PhC{\equiv}CC{\equiv}CPh$ and also with a different diyne, namely $SiMe_3C{\equiv}CC{\equiv}CSiMe_3$ (**2**).

---

[*] Corresponding author. Tel.: +61 8 83035939; fax: +61 8 83034358.

PII S0022-328X(98)00393-3

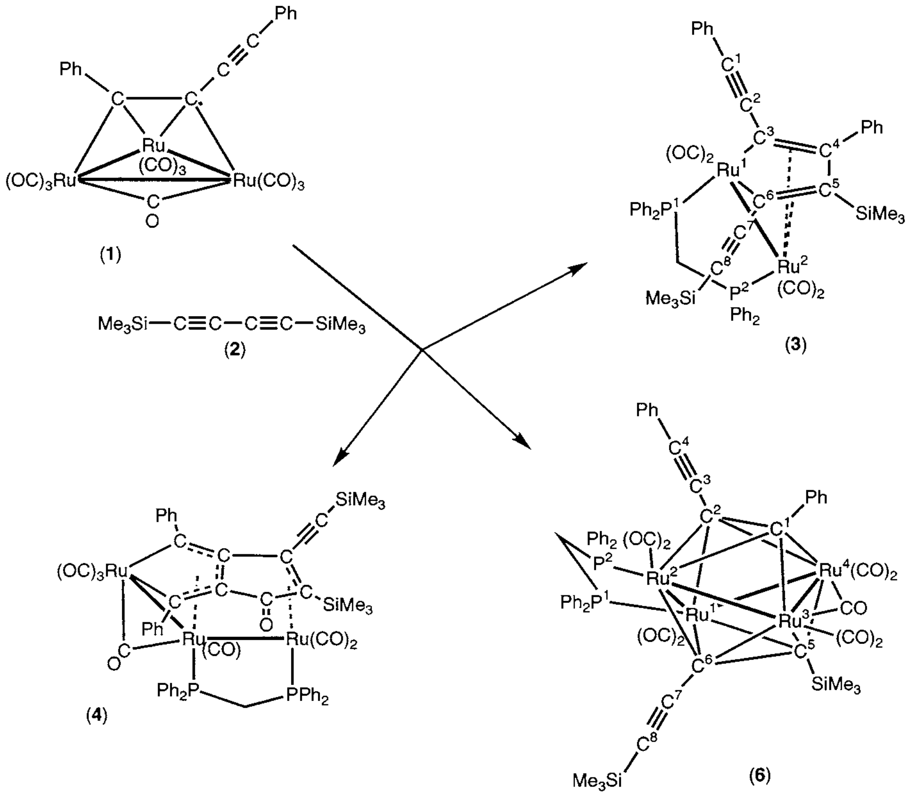

Scheme 1.

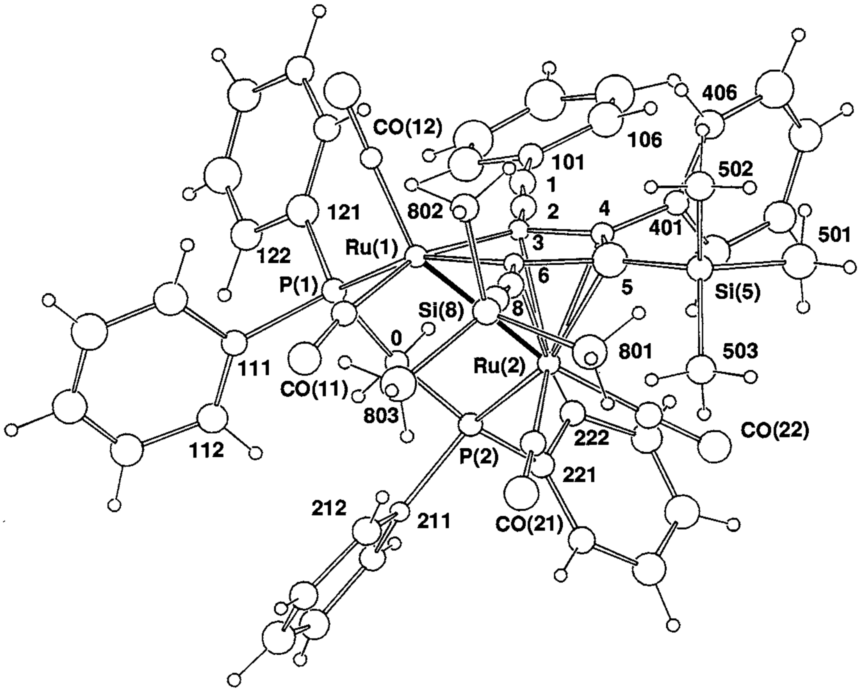

Fig. 1. Plot of a molecule of $Ru_2(\mu\text{-dppm})\{\mu\text{-C(C≡CPh)=CPhC(SiMe}_3\text{)=C(C≡CSiMe}_3\text{)}\}(CO)_4$ (**3**) in the orientation of Scheme 1, showing atom numbering system. In this and subsequent figures, non hydrogen atoms are shown with 20% thermal envelopes; hydrogen atoms have arbitrary radii of 0.1 Å.

Table 1
Selected bond lengths (Å) and angles (°) for $Ru_2(\mu\text{-dppm})\{\mu\text{-}C(C{\equiv}CPh)CPhC(SiMe_3)C(C{\equiv}CSiMe_3)\}(CO)_4$ (**3**)

Bond lengths (A)		Bond angles (°)	
Ru(1)–Ru(2)	2.724(4)	Ru(2)–Ru(1)–P(1)	100.3(2)
Ru(1)–P(1)	2.35(1)	Ru(1)–P(1)–C(0)	107.6(9)
Ru(2)–P(2)	2.31(1)	P(1)–C(0)–P(2)	115(2)
Ru(1)–C(3)	2.08(3)	C(0)–P(2)–Ru(2)	118(1)
Ru(1)–C(6)	1.94(3)	P(2)–Ru(2)–Ru(1)	87.0(2)
Ru(2)–C(3)	2.37(3)		
Ru(2)–C(4)	2.25(3)	C(3)–Ru(1)–C(6)	77(1)
Ru(2)–C(5)	2.28(4)	Ru(1)–C(3)–C(4)	116(2)
Ru(2)–C(6)	2.28(3)	C(3)–C(4)–C(5)	119(3)
P(1)–C(0)	1.84(3)	C(4)–C(5)–C(6)	96(2)
P(2)–C(0)	1.78(3)	C(5)–C(6)–Ru(l)	132(2)
Si(5)–C(5)	1.75(4)		
Si(8)–C(8)	1.85(4)	C(101)–C(1)–C(2)	174(3)
		C(1)–C(2)–C(3)	175(3)
		C(6)–C(7)–C(8)	170(3)
		C(7)–C(8)–Si(8)	171(3)

2. Results and discussion

These studies commenced when we found that during reactions of $Ru_3(\mu\text{-dppm})(CO)_{10}$ and $PhC{\equiv}CC{\equiv}CPh$, the first-formed $Ru_3(\mu_3\text{-}PhC_2C{\equiv}CPh)(\mu\text{-dppm})(CO)_8$ readily added a second molecule of the diyne, even at room temperature (r.t.). The product could be formulated as having two diynes attached to the Ru_3 core, but we have not yet obtained crystals suitable for an X-ray structure determination, as a result of the instability of this complex in solution.

However, we subsequently found that the reaction of **1** with $SiMe_3C{\equiv}CC{\equiv}CSiMe_3$ does not proceed at r.t., but when a mixture of the two components is heated in refluxing tetrahydrofuran for 2 h, up to five products can be separated (Scheme 1). Three complexes contain both PhC_2C_2Ph and $SiMe_3C_2C_2SiMe_3$ in various combinations. Two of these were readily identified as being products of thermolysis of **1**, one of which has been described before. All the complexes isolated from these reactions contained the unchanged dppm ligand bridging two of the ruthenium atoms.

Table 2
Selected bond lengths (Å) and angles (°) for $Ru_4(\mu_4\text{-}PhC_2C{\equiv}CPh)(\mu_4\text{-}SiMe_3C_2CSiMe_3)(\mu\text{-dppm})(\mu\text{-CO})(CO)_8$ (**6**)

Bond distances (Å)		Bond angles (°)	
Ru(1)–Ru(2)	2.822(8)	Ru(2)–Ru(1)–Ru(4)	86.2(2)
Ru(1)–Ru(4)	2.898(7)	Ru(1)–Ru(2)–Ru(3)	82.7(2)
Ru(2)–Ru(3)	2.873(7)	Ru(2)–Ru(3)–Ru(4)	88.6(2)
Ru(3)–Ru(4)	2.717(8)	Ru(1)–Ru(4)–Ru(3)	84.0(2)
Ru(1)–P(1)	2.27(2)	Ru(2)–Ru(1)–P(1)	85.5(5)
Ru(2)–P(2)	2.40(2)	Ru(1)–P(1)–C(0)	116(2)
Ru(1)–C(2)	2.23(5)	P(1)–C(0)–P(2)	114(3)
Ru(1)–C(5)	2.23(6)	C(0)–P(2)–Ru(2)	108(2)
Ru(1)–C(6)	2.21(5)	P(2)–Ru(2)–Ru(1)	96.5(5)
Ru(2)–C(1)	2.36(6)	Ru(3)–C(43)–O(43)	140(6)
Ru(2)–C(2)	2.30(5)	Ru(4)–C(43)–O(43)	135(6)
Ru(2)–C(6)	2.23(5)	C(101)–C(1)–C(2)	117(6)
Ru(3)–C(1)	2.16(6)	C(1)–C(2)–C(3)	126(5)
Ru(3)–C(5)	2.34(5)	C(2)–C(3)–C(4)	164(7)
Ru(3)–C(6)	2.31(6)	C(3)–C(4)–C(401)	173(6)
Ru(3)–C(43)	2.03(7)	Si(5)–C(5)–C(6)	131(4)
Ru(4)–C(43)	2.06(7)	C(5)–C(6)–C(7)	116(5)
Ru(4)–C(1)	2.27(6)	C(6)–C(7)–C(8)	172(8)
Ru(4)–C(2)	2.35(5)	C(7)–C(8)–Si(8)	171(6)
Ru(4)–C(5)	2.28(5)		

Pale yellow crystals of the dinuclear complex $Ru_2(\mu\text{-dppm})\{\mu\text{-}C(C{\equiv}CPh){=}CPhC(SiMe_3){=}C(C{\equiv}CSiMe_3)\}(CO)_4$ (**3**) were obtained in 34% yield. This complex was partially characterised from elemental analysis and its spectral properties and its molecular structure was determined by a single-crystal X-ray study. The IR ν(CO) spectrum contains four strong to very strong absorptions between 2021 and 1942 cm^{-1}, while a weak band at 2112 cm^{-1} is assigned to $\nu(C{\equiv}C)$. The proton NMR spectrum contains two signals at δ 0.13 and 0.23, assigned to two different $SiMe_3$ groups; the two CH_2 protons are found as multiplets at δ 4.58 and 5.25, while the Ph group resonates between δ 6.05 and 7.86. Unusually, we were not able to obtain a meaningful mass spectrum from **3**.

A plot of a molecule of **3** is shown in Fig. 1, with selected bond parameters being collected in Table 1. As can be seen, the complex is another example in the

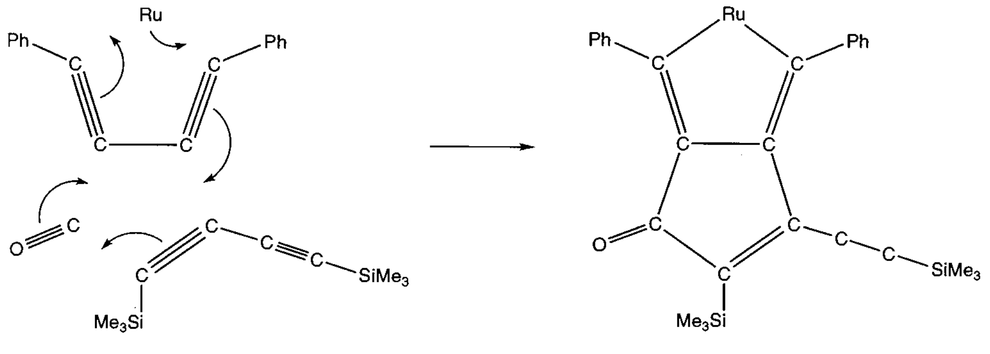

Scheme 2. Scheme 2

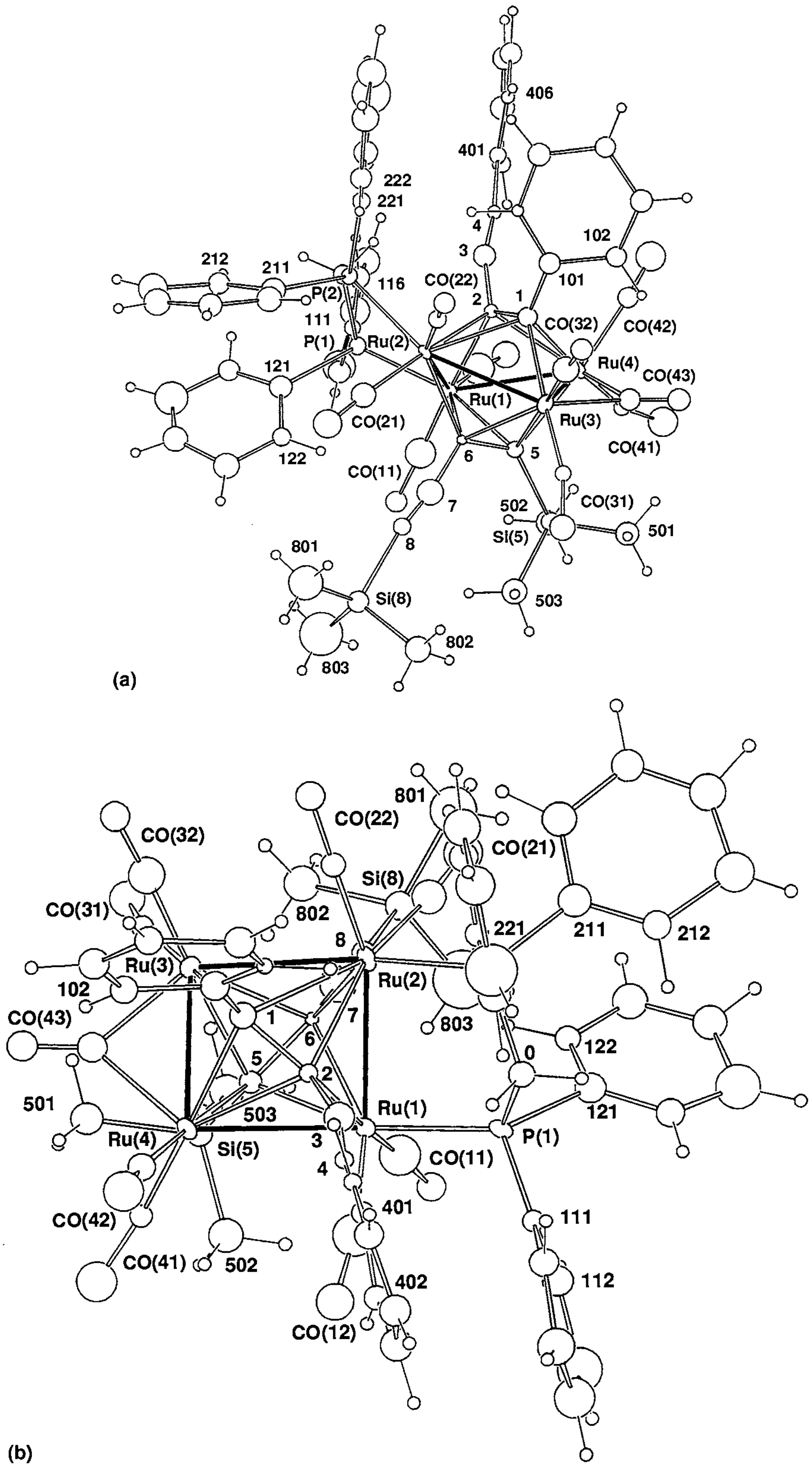

Fig. 2. (a) Plot of a molecule of $Ru_4(\mu_4\text{-}PhC_2C\equiv CPh)(\mu_4\text{-}SiMe_3C_2C\equiv CSiMe_3)(\mu\text{-dppm})(\mu\text{-}CO)(CO)_8$ (**6**), in the orientation of Scheme 1. (b) Projection of **6** normal to the Ru_4 'plane'.

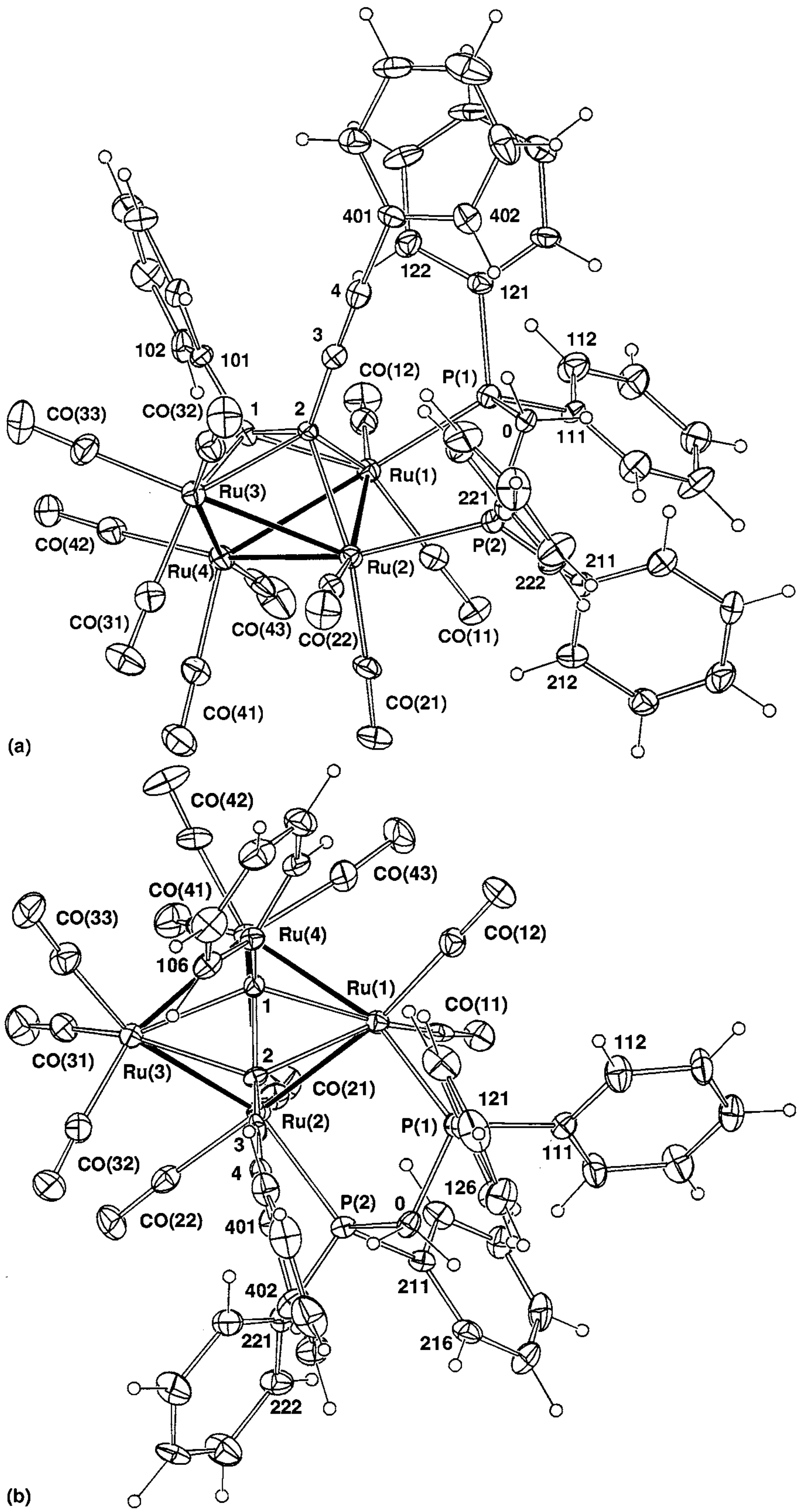

Fig. 3. (a) Plot of a molecule of $Ru_4(\mu_4\text{-}PhC_2C{\equiv}CPh)(\mu\text{-}dppm)(CO)_{10}$ (**7**) in the orientation of Scheme 1. (b) Projection of **7** from above the coordinated diyne.

Table 3
Selected bond lengths (Å) and angles (°) for $Ru_4(\mu_4\text{-}PhC_2C\equiv CPh)(\mu\text{-dppm})(CO)_{10}$ (**7**) and $Ru_4(\mu_4\text{-}PhC_2C\equiv CPh)(CO)_{12}$ (**8**)

Bond lengths (Å)	**7**	**8**	Bond angles (°)	**7**	**8**
Ru(1)–Ru(2)	2.712(2)	2.741(1)	Ru(2)–Ru(1)–P(1)	100.8(1)	–
Ru(1)–Ru(4)	2.747(2)	2.704(1)	Ru(1)–P(1)–C(0)	109.7(4)	–
Ru(2)–Ru(3)	2.743(2)	2.700(1)	P(1)–C(0)–P(2)	115.7(6)	–
Ru(2)–Ru(4)	2.863(3)	2.811(1)	C(0)–P(2)–Ru(2)	114.0(4)	–
Ru(3)–Ru(4)	2.706(2)	2.765(1)	P(2)–Ru(2)–Ru(1)	88.0(1)	–
Ru(1)–P(1)	2.280(4)	–	C(101)–C(1)–C(2)	122.9(9)	125.0(7)
Ru(2)–P(2)	2.351(4)	–	C(1)–C(2)–C(3)	122.5(9)	127.7(7)
Ru(1)–C(1)	2.25(1)	2.254(8)	C(2)–C(3)–C(4)	178(1)	175.9(9)
Ru(1)–C(2)	2.29(1)	2.208(8)	C(3)–C(4)–C(401)	176(1)	178.1(9)
Ru(2)–C(2)	2.19(1)	2.159(7)			
Ru(3)–C(1)	2.27(1)	2.231(8)			
Ru(3)–C(2)	2.23(1)	2.218(8)			
Ru(4)–C(1)	2.15(1)	2.137(7)			
P(1)–C(0)	1.84(1)	–			
P(2)–C(0)	1.85(1)	–			
C(1)–C(2)	1.46(2)	1.46(1)			
C(1)–C(101)	1.51(2)	1.50(1)			
C(2)–C(3)	1.41(1)	1.43(1)			
C(3)–C(4)	1.20(2)	1.19(1)			
C(4)–C(401)	1.46(2)	1.44(1)			

ruthenacyclopentadiene-$Ru(CO)_3$ series, the five-membered RuC_4 ring carrying substituents derived from the two diynes: Ph and $SiMe_3$ at atoms C(4) and C(5), while phenyl- and $SiMe_3$-alkynyl substituents are found at C(3) and C(6). The Ru(1)–Ru(2) bond [2.724(4) Å] is bridged by an intact dppm ligand and two CO groups are attached to each Ru atom.

The unsymmetrical attachment of the C(3)–C(4)–C(5)–C(6) unit to Ru(1) [Ru(1)–C(3, 6) 2.08, 1.94(3) Å] can be ascribed to the coordination of the dppm such that P(1) is opposite C(6), while C(3) is opposite a CO group. The precision of this determination does not allow us to comment on the degree of electron delocalisation around the diene group. However, preservation of the C≡C triple bonds between C(1)–C(2) and C(7)–C(8) is evidenced by the short separations between these atoms [both 1.23(5) Å].

The formation of **3** involves insertion of one C≡C triple bond of **2** into one of the Ru–C bonds of **1**, followed by degradation of the cluster by loss of an $Ru(CO)_3$ (?) group. In the course of this reaction, a straight-chain C_8 hydrocarbon is obtained by head-to head coupling of the diynes, as found with one of the products obtained from reactions between PhC≡CC≡CPh and $Ru_3(CO)_{10}(NCMe)_2$, namely Ru{C(C≡CPh)=CPhCPh=C(C≡CPh)}$(CO)_3(NMe_3)$ [2]. However, the binuclear derivative obtained from the same reaction has the head-to-tail coupled dimer in $Ru_2\{\mu$-CPh=C(C≡CPh)CPhC(CPh)$\}(CO)_6$ [2].

The fastest-moving complex on the t.1.c. plates is the red trinuclear $Ru_3\{\mu_3$-C($SiMe_3$)C(C≡C$SiMe_3$)C(=CPh)C(=CPh)C(O)$\}(\mu$-dppm)$(CO)_7$ (**4**). We have described the structure of this complex briefly on another occasion [8]. The organic ligand is formed by coupling PhC_2C_2Ph, $SiMe_2C_2C_2SiMe_3$ and CO molecules to give a novel bicyclic metallaindenone system. In this case, only the C≡C$SiMe_3$ substituent remains uncoordinated, a novel rearrangement of the diphenylbutadiyne system occurring so that the central two carbons of the C_4

Table 4
Crystal data and refinement details for complexes **3**, **6** and **7**

Compound	3	6	7
Formula	$C_{55}H_{50}O_4P_2Ru_2Si_2$ C_6H_6	$C_{60}H_{50}O_9P_2Ru_4Si_2$ C_6H_6	$C_{51}H_{32}O_{10}P_2Ru_4$ $0.5CH_2Cl_2$
Molecular weight	1173.4	1515.6	1313.5
Crystal system	Monoclinic	Monoclinic	Monoclinic
Space group	$P2_1/c$	$P2_1/c$	$P2_1/c$
Unit cell dimensions			
a (Å)	11.433(4)	20.128(8)	19.399(6)
b (Å)	10.894(9)	13.194(5)	11.119(10)
c (Å)	45.75(3)	24.514(5)	23.54(2)
β (°)	103.09(4)	97.36(3)	102.99(5)
V (Å^3)	5550	6456	4947
Z	4	4	4
D_{calc} (g cm^{-3})	1.404	1.559	1.763
$F(000)$	2400	3032	2580
Crystal size (mm)	0.05 × 0.15 × 0.11	0.14 × 0.07 × 0.07	0.16 × 0.40 × 0.06
A^* (min, max)	1.03, 1.07	1.06, 1.08	1.08, 1.27
μ (cm^{-1})	6.9	10.6	13.7
N	9757	8565	8686
N_o	2240	1413	4270
R	0.087	0.081	0.052
Rw	0.081	0.066	0.049

Table 5
Non-hydrogen positional and isotropic displacement parameters (**3**)

Atom	x	y	z	U_{eq} (Å^2)
Ru(1)	0.1245(2)	0.3819(3)	0.62442(6)	0.031(1)
Ru(2)	0.3172(2)	0.3000(3)	0.66639(6)	0.032(1)
C(11)	−0.005(3)	0.316(3)	0.6368(6)	0.040(9)
O(11)	−0.077(2)	0.264(2)	0.6470(5)	0.069(8)
C(12)	0.039(3)	0.495(3)	0.6020(7)	0.029(9)
O(12)	−0.022(2)	0.576(2)	0.5885(5)	0.080(9)
C(21)	0.257(3)	0.233(3)	0.6955(7)	0.04(1)
O(21)	0.213(2)	0.194(2)	0.7145(5)	0.075(8)
C(22)	0.468(3)	0.266(3)	0.6900(7)	0.05(1)
O(22)	0.564(2)	0.249(2)	0.7057(5)	0.067(8)
P(1)	0.1156(8)	0.2317(8)	0.5872(2)	0.037(4)
C(111)	−0.008(3)	0.126(3)	0.5801(6)	0.041(9)
C(112)	−0.003(3)	0.005(3)	0.5837(7)	0.06(1)
C(113)	−0.112(4)	−0.067(3)	0.5764(8)	0.07(1)
C(114)	−0.218(3)	−0.017(4)	0.5659(8)	0.07(1)
C(115)	−0.229(3)	0.105(4)	0.5631(8)	0.08(1)
C(116)	−0.125(3)	0.177(3)	0.5699(8)	0.07(1)
C(121)	0.118(3)	0.274(4)	0.5491(8)	0.07(1)
C(122)	0.101(3)	0.178(3)	0.5266(8)	0.06(1)
C(123)	0.105(3)	0.208(4)	0.4975(9)	0.08(1)
C(124)	0.114(3)	0.321(4)	0.4883(8)	0.07(1)
C(125)	0.131(3)	0.417(3)	0.5103(8)	0.05(1)
C(126)	0.130(3)	0.392(3)	0.5400(7)	0.044(9)
C(0)	0.250(2)	0.135(3)	0.5983(6)	0.034(9)
P(2)	0.3078(7)	0.1235(9)	0.6378(2)	0.035(4)
C(211)	0.221(3)	−0.008(3)	0.6453(6)	0.024(8)
C(212)	0.129(3)	−0.005(3)	0.6597(7)	0.05(1)
C(213)	0.054(3)	−0.110(3)	0.6615(7)	0.05(1)
C(214)	0.081(3)	−0.215(4)	0.6481(8)	0.07(1)
C(215)	0.180(3)	−0.226(3)	0.6348(7)	0.06(1)
C(216)	0.243(2)	−0.117(3)	0.6333(6)	0.041(9)
C(221)	0.458(3)	0.063(3)	0.6421(7)	0.04(1)
C(222)	0.531(3)	0.108(3)	0.6245(6)	0.041(9)
C(223)	0.661(3)	0.085(3)	0.6331(8)	0.06(1)
C(224)	0.704(3)	0.018(4)	0.6580(9)	0.07(1)
C(225)	0.631(3)	−0.037(3)	0.6752(8)	0.07(1)
C(226)	0.510(3)	−0.006(3)	0.6670(7)	0.05(1)
C(1)	0.408(3)	0.394(3)	0.5793(7)	0 043(9)
C(101)	0.477(3)	0.381(3)	0.5559(7)	0.039(9)
C(102)	0.436(3)	0.310(4)	0.5325(9)	0.07(1)
C(103)	0.503(4)	0.296(4)	0.5101(9)	0.09(1)
C(104)	0.601(4)	0.367(4)	0.512(1)	0.10(2)
C(105)	0.650(3)	0.435(4)	0.536(1)	0.09(2)
C(106)	0.580(3)	0.449(4)	0.5588(8)	0.08(1)
C(2)	0.361(3)	0.405(3)	0.6007(7)	0.040(9)
C(3)	0.301(2)	0.420(3)	0.6223(7)	0.027(8)
C(4)	0.375(3)	0.478(3)	0.6490(6)	0.032(9)
C(401)	0.494(3)	0.527(3)	0.6477(7)	0.037(9)
C(402)	0.593(3)	0.445(3)	0.6490(8)	0.07(1)
C(403)	0.703(3)	0.494(4)	0.6452(8)	0.06(1)
C(404)	0.709(3)	0.617(4)	0.6387(7)	0.07(1)
C(405)	0.619(4)	0.695(4)	0.6383(8)	0.09(1)
C(406)	0.512(3)	0.647(3)	0.6427(7)	0.05(1)
C(5)	0.319(3)	0.504(3)	0.6775(9)	0.08(1)
Si(5)	0.3836(8)	0.5733(9)	0.7118(2)	0.042(4)
C(501)	0.545(3)	0.596(4)	0.7169(8)	0.08(1)
C(502)	0.313(3)	0.721(3)	0.7147(7)	0.05(1)
C(503)	0.364(3)	0.475(3)	0.7425(7)	0.05(1)
C(6)	0.190(2)	0.463(3)	0.6625(6)	0.025(8)
C(7)	0.123(3)	0.486(3)	0.6868(7)	0.04(1)
C(8)	0.053(3)	0.503(3)	0.7032(7)	0.05(1)
Si(8)	−0.0380(8)	0.549(1)	0.7299(2)	0.047(5)
C(801)	0.070(3)	0.567(3)	0.7665(8)	0.07(1)
C(802)	−0.113(3)	0.692(3)	0.7163(7)	0.05(1)
C(803)	−0.149(3)	0.428(3)	0.7311(8)	0.08(1)
C(01)	0.421(4)	−0.079(4)	0.549(1)	0.10(2)
C(02)	0.428(4)	−0.166(5)	0.567(1)	0.12(2)
C(03)	0.337(5)	−0.252(5)	0.566(1)	0.14(2)
C(04)	0.240(4)	−0.238(4)	0.547(1)	0.11(2)
C(05)	0.222(4)	−0.150(4)	0.5245(9)	0.09(1)
C(06)	0.316(4)	−0.065(4)	0.528(1)	0.11(2)

chain are involved in the cyclisation, with exocyclic =CPh groups being attached to the Ru atoms. Incorporation of the CO ligand to form a five-membered cyclopentadienone ring is a common feature of metal carbonyl-alkyne chemistry. The organic ligand on this cluster is formed by a series of insertion reactions, which may be represented as shown in Scheme 2, which depicts a series of reactions which are mediated by the cluster. Involvement of the second C≡C triple bond of the PhC≡CC≡CPh ligand in a reaction on a trinuclear cluster is a notable feature: at some stage, opening of the cluster may facilitate coordination of this bond and subsequent coupling with the silylated diyne and CO.

A second trinuclear complex was identified as $Ru_3\{\mu_3\text{-CPhCHCC}(C_6H_4)\}(\mu\text{-dppm})(CO)_8$ (**5**), which was obtained previously by thermolysis of **1**, the likely source of it on this occasion [7].

Two tetranuclear complexes were also isolated from the reaction products. The first formed red–orange crystals which were identified as $Ru_4(\mu_4\text{-PhC}_2C{\equiv}CPh)(\mu_4\text{-SiMe}_3C_2C{\equiv}CSiMe_3)(\mu\text{-dppm})(\mu\text{-CO})(CO)_8$ (**6**) by the single-crystal X-ray structure determination. The IR ν(CO) spectrum contained a plethora of bands in the region between 2063 and 1899 cm^{-1}, together with a weak absorption at 1823 cm^{-1}, assigned to the bridging CO ligand found in the structural determination. In the FAB mass spectrum, the highest mass ion corresponds to [M-2CO]$^+$.

Fig. 2 shows a plot of a molecule of **6**, significant bond distances and angles being in Table 2. The four Ru atoms form a rhomboid bent about the diagonals to form an open butterfly. The Ru–Ru separations range from 2.717(8) to 2.898(7) Å, the shortest being symmetrically bridged by CO(43). The Ru(1)–Ru(2) separation is also short at 2.822(8) Å, and is asymmetrically bridged by the dppm ligand, with Ru–P distances of 2.27, 2.40(2) Å and corresponding differences in the Ru–Ru–P [85.5, 96.5(5)°] and Ru–P–C(0) angles [116, 108(2)°]. The two longer, non-bridged Ru–Ru vectors are 2.873, 2.898(7) Å.

A molecule of each diyne is attached to all four metal atoms by means of one of its C≡C triple bonds, so that the C_4Ru_4 skeleton forms a distorted antiprism. The

Table 6
Non-hydrogen positional and isotropic displacement parameters (**6**)

Atom	x	y	z	U_{eq} (Å^2)
Ru(1)	0.6601(3)	0.8480(4)	0.6849(2)	0.026(2)
Ru(2)	0.8001(3)	0.8191(4)	0.6948(2)	0.027(3)
Ru(3)	0.7860(3)	0.9268(4)	0.5921(2)	0.034(3)
Ru(4)	0.6835(3)	1.0331(4)	0.6266(2)	0.029(3)
C(11)	0.609(4)	0.759(6)	0.661(3)	0.11(3)
O(11)	0.561(2)	0.690(3)	0.646(1)	0.05(1)
C(12)	0.592(4)	0.926(7)	0.704(3)	0.12(4)
O(12)	0.551(2)	0.986(4)	0.711(2)	0.08(2)
C(21)	0.820(4)	0.689(6)	0.687(3)	0.07(3)
O(21)	0.836(3)	0.608(4)	0.679(2)	0.09(2)
C(22)	0.885(3)	0.847(5)	0.694(2)	0.04(2)
O(22)	0.944(2)	0.858(3)	0.689(1)	0.05(1)
C(31)	0.789(3)	0.879(4)	0.525(2)	0.03(2)
O(31)	0.786(2)	0.823(4)	0.482(2)	0.08(2)
C(32)	0.871(4)	0.968(6)	0.588(3)	0.08(3)
O(32)	0.926(2)	0.996(3)	0.583(1)	0.05(2)
C(41)	0.607(3)	1.071(5)	0.592(2)	0.03(2)
O(41)	0.557(2)	1.123(4)	0.571(2)	0.10(2)
C(42)	0.691(3)	1.170(5)	0.658(2)	0.05(2)
O(42)	0.693(3)	1.241(4)	0.678(2)	0.10(2)
C(43)	0.739(3)	1.055(5)	0.562(3)	0.06(2)
O(43)	0.746(2)	1.119(3)	0.534(2)	0.06(2)
P(1)	0.6666(9)	0.771(1)	0.7683(7)	0.032(8)
C(111)	0.604(3)	0.799(5)	0.801(2)	0.03(2)
C(112)	0.538(4)	0.753(5)	0.788(2)	0.06(2)
C(113)	0.475(5)	0.775(7)	0.808(3)	0.12(4)
C(114)	0.479(4)	0.851(7)	0.844(3)	0.10(3)
C(115)	0.540(4)	0.901(6)	0.863(3)	0.09(3)
C(116)	0.595(3)	0.861(5)	0.841(3)	0.05(2)
C(121)	0.671(3)	0.627(5)	0.774(3)	0.06(2)
C(122)	0.687(3)	0.573(5)	0.729(2)	0.04(2)
C(123)	0.696(3)	0.470(6)	0.732(3)	0.08(2)
C(124)	0.686(3)	0.433(5)	0.784(3)	0.07(3)
C(125)	0.654(4)	0.477(7)	0.827(3)	0.13(3)
C(126)	0.653(3)	0.582(6)	0.820(3)	0.05(2)
C(0)	0.736(3)	0.806(5)	0.817(2)	0.04(2)
P(2)	0.8164(8)	0.793(1)	0.7922(7)	0.028(8)
C(211)	0.851(4)	0.670(5)	0.813(3)	0.07(2)
C(212)	0.829(3)	0.612(5)	0.852(3)	0.05(2)
C(213)	0.858(4)	0.512(6)	0.876(3)	0.10(3)
C(214)	0.912(4)	0.490(5)	0.849(3)	0.08(3)
C(215)	0.937(3)	0.551(6)	0.812(3)	0.06(2)
C(216)	0.907(4)	0.641(6)	0.794(3)	0.07(3)
C(221)	0.874(3)	0.870(4)	0.832(2)	0.04(2)
C(222)	0.941(4)	0.875(5)	0.834(3)	0.05(2)
C(223)	0.988(4)	0.929(6)	0.869(3)	0.08(3)
C(224)	0.965(4)	0.989(6)	0.908(3)	0.10(3)
C(225)	0.893(6)	0.986(8)	0.908(4)	0.17(4)
C(226)	0.849(3)	0.930(5)	0.875(3)	0.07(3)
C(1)	0.785(3)	0.993(5)	0.673(2)	0.04(2)
C(101)	0.832(3)	1.064(5)	0.693(3)	0.05(2)
C(102)	0.840(3)	1.157(5)	0.660(2)	0.05(2)
C(103)	0.886(3)	1.235(5)	0.681(3)	0.06(2)
C(104)	0.921(3)	1.232(5)	0.735(3)	0.05(2)
C(105)	0.909(3)	1.141(5)	0.767(2)	0.06(2)
C(106)	0.865(3)	1.067(4)	0.744(2)	0.01(2)
C(2)	0.740(3)	0.963(4)	0.708(2)	0.02(2)
C(3)	0.729(3)	1.013(5)	0.759(3)	0.06(2)
C(4)	0.716(3)	1.073(4)	0.792(2)	0.02(2)
C(401)	0.700(3)	1.139(4)	0.840(2)	0.03(2)
C(402)	0.633(3)	1.153(4)	0.847(2)	0.04(2)
C(403)	0.622(3)	1.213(5)	0.895(3)	0.07(3)
C(404)	0.668(4)	1.254(5)	0.922(3)	0.06(2)
C(405)	0.728(4)	1.252(5)	0.908(3)	0.05(2)
C(406)	0.749(3)	1.198(4)	0.869(2)	0.02(2)
Si(5)	0.612(1)	0.858(2)	0.5354(8)	0.042(6)
C(501)	0.627(3)	0.943(5)	0.481(2)	0.06(2)
C(502)	0.534(3)	0.874(5)	0.555(2)	0.07(3)
C(503)	0.610(3)	0.740(5)	0.499(2)	0.07(3)
C(5)	0.677(3)	0.869(4)	0.598(2)	0.03(2)
C(6)	0.723(3)	0.798(4)	0.622(2)	0.01(2)
C(7)	0.722(4)	0.702(6)	0.596(3)	0.08(3)
C(8)	0.727(3)	0.629(5)	0.582(2)	0.03(2)
Si(8)	0.726(1)	0.496(2)	0.5450(8)	0.052(7)
C(801)	0.798(4)	0.427(6)	0.570(3)	0.14(4)
C(802)	0.730(3)	0.525(5)	0.474(2)	0.08(2)
C(803)	0.653(5)	0.433(8)	0.557(4)	0.21(5)
C(01)	0.999(5)	0.749(6)	0.560(3)	0.11(3)
C(02)	1.070(7)	0.764(9)	0.559(5)	0.20(6)
C(03)	1.081(7)	0.78(1)	0.513(7)	0.24(7)
C(04)	1.027(6)	0.783(7)	0.469(4)	0.14(4)
C(05)	0.958(4)	0.767(5)	0.478(3)	0.09(3)
C(06)	0.937(5)	0.729(6)	0.530(4)	0.13(4)

alkynyl substituents are each on the carbons σ-bonded to the Ru atoms bridged by the dppm ligand. The bonding is similar to that found in complexes of the type $Ru_4(\mu_4\text{-}C_2R_2)(CO)_{12}$, in which the hinge bond of the butterfly is retained (see below). The alkynes are each attached via one of the C≡C triple bonds in the 2σ, 2π fashion. There is little significant difference between the Ru–C σ bonds, which range between 2.16–2.28(5) A (av. 2.23 A), and the Ru–C σ bonds [2.21–2.36(6) Å, av. 2.30 Å]. The C–C separations for the coordinated alkynes are both 1.39(7) Å while the free C≡C triple bonds are 1.19(9) Å (Ph) and 1.0(1) Å ($SiMe_3$). The bend-back angles at the coordinated alkyne carbons are between 116 and 131(4)°, although the uncoordinated C≡C units are almost linear [164–173(6)°].

The only previous examples of complexes of this type appear to be $Ru_4(\mu_4\text{-}MeC_2Ph)(\mu_4\text{-alkyne})(CO)_{11}$ (alkyne = HC_2H, HC_2But, EtC_2Et and MeC_2Ph), obtained from reactions of $Ru_4(\mu_4\text{-}MeC_2Ph)(CO)_{12}$ with the appropriate alkynes: the crystal structure of the latter was determined [9]. These observations point to a likely route to **6**, the reaction between $SiMe_3C{\equiv}CC{\equiv}CSiMe_3$ and $Ru_4(\mu_4\text{-}PhC_2C{\equiv}CPh)(\mu\text{-dppm})(CO)_{10}$ (**7**) (below), also isolated from this reaction. The C_4Ru_4 skeleton of **6** is also present in $Fe_2Ru_6(\mu_6\text{-}C_2)_2(CO)_{17}Cp^*_2$, obtained from reactions between $Ru_3(CO)_{12}$ and $\{Fe(CO)_2Cp^*\}_2(\mu\text{-}C_2)$ [10].

The second tetranuclear complex contains no silylated diyne and can be considered to be another thermolysis product of **1**, although we did not find it in our earlier study [9]. This compound (**7**), which forms dark red crystals, was readily identified as the dppm-substitution product of $Ru_4(\mu_4\text{-}PhC_2C{\equiv}CPh)(CO)_{12}$ (**8**) The

Table 7
Non-hydrogen positional and isotropic displacement parameters (**7**)

Atom	x	y	z	U_{eq} (Å^2)
Ru(l)	0.81813(5)	0.43641(9)	0.61240(4)	0.0348(3)
Ru(2)	0.72262(5)	0.48693(9)	0.67729(4)	0.0344(3)
Ru(3)	0.62209(5)	0.34038(9)	0.61103(4)	0.0397(4)
Ru(4)	0.75210(5)	0.24380(9)	0.65047(4)	0.0390(4)
C(11)	0.8846(6)	0.459(1)	0.6805(5)	0.043(5)
O(11)	0.9292(4)	0.4708(8)	0.7226(3)	0.056(4)
C(12)	0.8835(6)	0.372(1)	0.5719(5)	0.049(5)
O(12)	0.9269(5)	0.3309(8)	0.5525(4)	0.067(4)
C(21)	0.7647(6)	0.451(1)	0.7542(5)	0.046(5)
O(21)	0.7908(5)	0.4237(8)	0.8018(3)	0.069(4)
C(22)	0.6402(7)	0.531(1)	0.7016(5)	0.050(5)
O(22)	0.5922(5)	0.5614(9)	0.7199(4)	0.078(5)
C(31)	0.5935(6)	0.279(1)	0.6769(6)	0.055(5)
O(31)	0.5754(5)	0.2448(9)	0.7172(4)	0.082(5)
C(32)	0.5478(6)	0.451(1)	0.5865(6)	0.056(6)
O(32)	0.5045(5)	0.5226(9)	0.5723(4)	0.081(5)
C(33)	0.5750(7)	0.217(1)	0.5623(6)	0.062(6)
O(33)	0.5500(5)	0.1414(9)	0.5327(5)	0.090(5)
C(41)	0.7437(7)	0.189(1)	0.7252(5)	0.047(5)
O(41)	0.7383(5)	0.1547(9)	0.7700(4)	0.077(5)
C(42)	0.7246(7)	0.097(1)	0.6125(5)	0.054(5)
O(42)	0.7103(6)	0.0105(8)	0.5875(4)	0.086(5)
C(43)	0.8497(7)	0.203(1)	0.6677(6)	0.056(6)
O(43)	0.9066(5)	0.1703(9)	0.6768(5)	0.090(5)
P(1)	0.8397(2)	0.6242(3)	0.5816(1)	0.037(1)
C(111)	0.9313(6)	0.671(1)	0.6018(5)	0.039(4)
C(112)	0.9766(7)	0.634(1)	0.5674(5)	0.064(6)
C(113)	1.0483(6)	0.658(1)	0.5830(6)	0.064(6)
C(114)	1.0753(7)	0.723(1)	0.6326(6)	0.065(6)
C(115)	1.0313(7)	0.760(1)	0.6676(5)	0.071(6)
C(116)	0.9591(6)	0.735(1)	0.6502(6)	0.061(6)
C(121)	0.8186(6)	0.652(1)	0.5033(5)	0.036(4)
C(122)	0.8019(6)	0.559(1)	0.4635(5)	0.047(5)
C(123)	0.7869(7)	0.582(1)	0.4043(5)	0.068(6)
C(124)	0.7874(7)	0.698(1)	0.3859(5)	0.068(6)
C(125)	0.8034(8)	0.792(1)	0.4240(6)	0.068(6)
C(126)	0.8192(7)	0.769(1)	0.4845(5)	0.054(5)
C(0)	0.7863(6)	0.735(1)	0.6103(5)	0.039(4)
P(2)	0.7572(2)	0.6895(3)	0.6769(1)	0.036(1)
C(211)	0.8270(6)	0.757(1)	0.7335(5)	0.037(4)
C(212)	0.8672(6)	0.688(1)	0.7780(5)	0.049(5)
C(213)	0.9212(6)	0.743(1)	0.8196(5)	0.053(5)
C(214)	0.9327(7)	0.862(1)	0.8165(6)	0.064(6)
C(215)	0.8945(7)	0.931(1)	0.7737(6)	0.062(6)
C(216)	0.8422(6)	0.878(1)	0.7323(5)	0.047(5)
C(221)	0.6821(6)	0.790(1)	0.6754(5)	0.040(5)
C(222)	0.6779(7)	0.862(1)	0.7228(5)	0.053(5)
C(223)	0.6173(7)	0.931(1)	0.7206(6)	0.073(6)
C(224)	0.5617(7)	0.927(1)	0.6739(7)	0 074(7)
C(225)	0.5642(7)	0.850(1)	0.6272(6)	0.070(6)
C(226)	0.6248(7)	0.783(1)	0.6294(5)	0.054(5)
C(101)	0.7086(6)	0.292(1)	0.5089(4)	0.033(4)
C(102)	0.7582(7)	0.215(1)	0.4943(5)	0.051(5)
C(103)	0.7543(7)	0.174(1)	0.4389(6)	0.063(6)
C(104)	0.6967(8)	0.211(1)	0.3941(6)	0.069(7)
C(105)	0.6452(7)	0.282(1)	0.4078(5)	0.065(6)
C(106)	0.6520(7)	0.321(1)	0.4650(5)	0.048(5)
C(1)	0.7177(6)	0.341(1)	0.5701(5)	0.035(4)
C(2)	0.6983(6)	0.4637(9)	0.5825(4)	0.029(4)
C(3)	0.6717(5)	0.548(1)	0.5379(5)	0.035(4)
C(4)	0.6496(6)	0.622(1)	0.5012(5)	0.041(5)
C(401)	0.6283(6)	0.712(1)	0.4558(5)	0.042(5)
C(402)	0.6288(7)	0.833(1)	0.4714(6)	0.062(6)
C(403)	0.6168(8)	0.919(1)	0.4285(7)	0.079(7)
C(404)	0.6042(8)	0.887(2)	0.3706(7)	0.089(8)
C(405)	0.6023(7)	0.768(1)	0.3555(5)	0.071(6)
C(406)	0.6140(6)	0.679(1)	0.3979(5)	0.055(5)
Cl	1.0443(6)	0.9734(9)	0.4632(6)	0.37(1)
C(01)[a]	0.955(3)	0.991(5)	0.459(2)	0.21(2)

[a] Site occupancy factor = 0.5.

IR spectrum contains several bands between 2069 and 1937 cm^{-1} and the FAB mass spectrum contains M$^+$ at m/z 1272, which fragments by loss of up to ten CO groups. The molecular structure was confirmed by a single-crystal X-ray study.

Fig. 3 is a plot of a molecule of **7** and some bond parameters are given in Table 3, together with corresponding values for **8**. As can be seen, the dppm ligand bridges Ru(1)–Ru(2), i.e. the vector joining a wing-tip atom to a hinge atom in the butterfly. Again, the Ru–P bonds differ significantly, the shorter being Ru(1)–P(1) [2.280(4) Å], while that to the Ru which is σ-bonded to the alkyne is 2.351(4) Å.

The Ru–Ru separations range between 2.706 and 2.863(3) Å, the longest being the hinge bond. The average length of the other four ‘outer’ bonds is 2.73 Å. As found in the parent compound, the Ru_4 butterfly is distorted so that opposite edges have similar lengths, although the pairs of Ru–Ru separations differ by ca. 0.04 Å.

The diyne is attached by only one of its C≡C triple bonds, as found in **6**, with σ bonds to Ru(2) and Ru(4) [2.15, 2.19(1) Å] and π-type bonds to the wing-tip Ru atoms [2.23–2.29(1) Å]. The coordinated C–C separation is 1.46(2) Å, while the ‘free’ C≡C triple bond is 1.20(2) Å. Bend-back angles at C(1) and C(2) are 122.9(9) and 122.5(9)°, respectively. We note an interesting relative orientation of Ph(40) and Ph(12) which are almost eclipsed with a ring plane separation of ca. 3.5 Å. Comparison with the structure of **8** shows the major difference to be a lengthening of the hinge bond by ca. 0.05 Å. There is essentially no other significant change in bonding parameters for similar bonds.

3. Conclusions

This limited study of the reactions of **1** with $SiMe_3C{\equiv}CC{\equiv}CSiMe_3$ has shown the existence of addition and cluster degradation or redistribution reactions to occur, the simple head-to-head dimer being found in the dinuclear complex **3**. In trinuclear **4**, incorporation of CO is also found, together with the unusual involvement of all four of the orginal dinye carbons of **1** in bonding to only two of the Ru atoms. Finally, tetranuclear **6** contains both diynes, but these are found on opposite sides of the cluster and have not coupled.

4. Experimental

General experimental conditions and instrumentation were similar to those as described in previous papers. Literature methods were used to prepare $Ru_3(\mu_3\text{-}PhC_2C{\equiv}CPh)(\mu\text{-dppm})(CO)_8$ [7] and $SiMe_3C{\equiv}CCSiMe_3$ [11].

*4.1. Reaction between $Ru_3(\mu_3\text{-}PhC_2C{\equiv}CPh)(\mu\text{-dppm})(CO)_8$ (**1**) and $SiMe_3C{\equiv}CC{\equiv}CSiMe_3$*

A mixture of 1 (68 mg, 0.061 mmol) and the diyne (24 mg, 0.122 mmol) was heated in refluxing tetrahydrofuran (10 ml) for 2 h. After this time, TLC showed the disappearance of **1** and the formation of several new bands. After cooling, solvent was removed and the residue, dissolved in the minimum amount of CH_2Cl_2, was separated by preparative TLC (silica, acetone/hexane 3/7) into five bands and a baseline, which was not further investigated.

From the first band (R_f 0.50) a red solid was isolated. Crystallisation (CH_2Cl_2/EtOH) gave red crystals of $Ru_3\{\mu_3\text{-}C(SiMe_3)C(C{\equiv}CSiMe_3)C(CPh)C(CPh)C(O)\}(\mu\text{-dppm})(CO)_7$ (**4**) (9.1 mg, 11.4%) as the hemi-CH_2Cl_2 solvate. Anal. Found: C, 53.43; H, 3.87. $C_{59}H_{50}O_8P_2Ru_3Si_2\cdot0.5CH_2Cl_2$ calcd: C, 52.93; H, 3.78%. IR (cyclohexane): ν(CC) 2164w; ν(CO) 2079s, 2019m, 2010vs, 1978m, 1968(sh), 1948w, 1893w(br) cm^{-1}. ^{1}H-NMR ($CDCl_3$): δ 0.01 (s, 9H, $SiMe_3$), 0.18 (s, 9H, $SiMe_3$), 3.51 [t, 2H, J(PH) = 11 Hz, CH_2], 6.27–7.59 (m, 30H, Ph). FAB mass spectrum (m/z): 1281, $[M\text{-}CO]^+$; 1253–1113, $[M\text{-}nCO]^+$ ($n = 2$–7); 1036, $[M\text{-}7CO\text{-}Ph]^+$.

The product from band 2 (R_f 0.38) was recrystallised from benzene to give pale yellow crystals of $Ru_2(\mu\text{-dppm})\{\mu\text{-}C(C{\equiv}CPh)CPhC(SiMe_3)C(C{\equiv}CSiMe_3)\}(CO)_4$ (**3**) (24.7 mg, 34.5%), obtained as the benzene solvate. Anal. Found: C, 62.34; H, 4.47. $C_{55}H_{50}O_4P_2Ru_2Si_2\cdot C_6H_6$ calcd: C, 62.46; H, 4.78%. IR (cyclohexane): ν(CC) 2112w; ν(CO) 2021s, 2002vs, 1971s, 1960w, 1942vs, 1904vw cm^{-1}. ^{1}H-NMR ($CDCl_3$): δ 0.13 (s, 9H, $SiMe_3$), 0.23 (s, 9H, $SiMe_3$), 4.58 (m, 1H, CH_2), 5.25 [dt, 1H, J(PH) = 12, J(HH) = 13 Hz, CH2], 6.05–7.86 (m, 30H, Ph). This complex did not give a satisfactory mass spectrum.

Band 3 (yellow, R_f 0.33) afforded the known $Ru_3\{\mu_3\text{-}CPhCHCC(C_6H_4)\}(\mu\text{-dppm})(CO)_8$ (**5**) (4 mg, 6%) as yellow crystals (from CH_2Cl_2/MeOH), identified from its IR ν(CO) spectrum and by a second X-ray structural study.

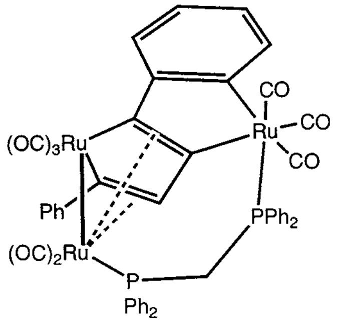

(5)

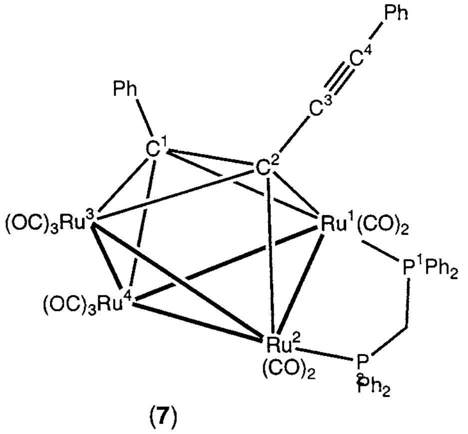

(7)

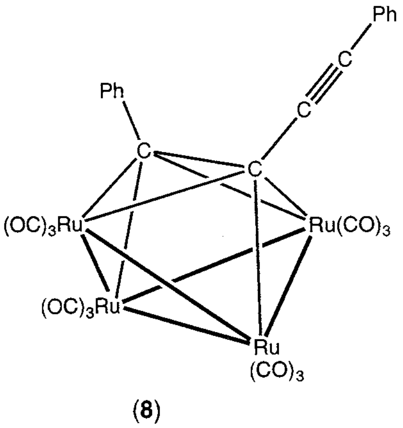

(8)

Band 4 (purple, R_f 0.27) gave very dark red crystals (from C_6H_6/hexane or CH_2Cl_2/EtOH) of $Ru_4(\mu_4$-$PhC_2C{\equiv}CPh)(\mu$-dppm$)(CO)_{10}$ (**7**) (8 mg, 10%). Anal. Found: C, 48.18; H, 2.54. $C_{51}H_{32}O_{10}P_2Ru_4$ calcd: C, 48.19; H, 2.51%. IR (cyclohexane): ν(CO) 2069s, 2054vw, 2034vs, 2007vs, 1988m, 1976m, 1956m, 1937m cm^{-1}. ^{1}H-NMR ($CDCl_3$): δ 4.44 (dt, 1H, CH_2), 5.12 (m, 1H, CH_2), 6.37–7.38 (m, 30H, Ph). FAB mass spectrum (m/z): 1272, M^+; 1244–992, [M-nCO] + (n = 1–10), 915, $[M\text{-}10CO\text{–}Ph]^+$.

Red–orange crystals (from C_6H_6) of $Ru_4(\mu_4$-$PhC_2C{\equiv}CPh)(\mu_4SiMe_3C_2C{\equiv}CSiMe_3)(\mu$-dppm$)(\mu$-CO$)(CO)_8$ (**6**) (3.1 mg, 3.6%) were obtained from band 5 (R_f 0.20). IR (cyclohexane): ν(CO) 2063vw, 2044w, 2024vs, 2013m, 2002m, 1982m, 1968w, 1958w, 1946w, 1899vw, 1823w cm^{-1}. FAB mass spectrum (m/z): 1382, $[M\text{-}2CO]^+$; 1354–1186, [M-nCO] + (n = 3–9). The structure of this complex was determined from the X-ray crystallographic study.

4.2. Crystallography

Unique data sets were measured at ca. 295 K using an Enraf-Nonius CAD4 diffractometer ($2\theta/\theta$ scan mode; $2\theta_{max} = 50°$; monochromatic Mo–K_α radiation, λ 0.71073 Å); N independent reflections were obtained N_o with $I > 3\sigma(I)$ being considered observed and used in the full matrix least squares refinement after gaussian absorption correction. Anisotropic thermal parameters were refined for the non-hydrogen atoms; $(x, y, z, U_{iso})_H$ were included constrained at estimated values. Conventional residuals R, R' on $|F|$ are quoted, statistical weights derivative of $\sigma^2(I) = \sigma^2(I_{diff}) + 0.0004\sigma^4\text{-}(I_{diff})$ being used. Computation used the XTAL 3.2 program system [12] implemented by S.R. Hall; neutral atom complex scattering factors were employed. Crystal data and refinement details are given in Table 4; other pertinent details are given in the Tables 5–7 and Figures.

4.3. Abnormal features and variations in procedure

Available crystals of all materials in the present study were small, those of **3** and **6** in particular, severely limiting the accessible data and the precision of the determinations, supporting meaningful anisotropic thermal parameter refinement for Ru, P and S only. In **3** and **7**, solvent occupancies were constrained at 1.0, 0.5, respectively, after trial refinement.

Acknowledgements

We thank the Australian Research Council for support of this work and Johnson Matthey Technology plc, Reading, UK, for a generous loan of $RuCl_3 \cdot nH_2O$.

References

[1] A.K. Smith, in E.W. Abel, F.G.A. Stone, G. Wilkinson (Eds.), Comprehensive Organometallic Chemistry 11,vol. 7, Elsevier, Oxford, 1995, p. 747.

[2] M.I. Bruce, N.N. Zaitseva, B.W. Skelton, A.H. White, Inorg. Chim. Acta 250 (1996) 129.

[3] A.J. Deeming, M.S.B. Felix, D. Nuel, Inorg. Chim. Acta 213 (1993) 3.

[4] M.I. Bruce, N.N. Zaitseva, B.W. Skelton, A.H. White, J. Cluster Sci. 7 (1996) 109.

[5] J.F. Corrigan, S. Doherty, N.J. Taylor, A.J. Carty, Organometallics 11 (1992) 3160.

[6] J.F. Corrigan, N.J. Taylor, A.J. Carty, Organometallics 13 (1994) 3778.

[7] M.I. Bruce, N.N. Zaitseva, B.W. Skelton, A.H. White, J. Organomet. Chem. 536–537 (1997) 93.

[8] M.I. Bruce, N.N. Zaitseva, B.W. Skelton, A.H. White, lzv. Akad. Nauk Ross., Ser. Khim. (in press).

[9] S. Aime, G. Nicola, D. Osella, A.M. Manotti Lanfredi, A. Tiripicchio, Inorg. Chim. Acta 85 (1984) 161.

[10] M. Akita, S. Sugimoto, M. Tanaka, Y. Moro-oka, J. Am. Chem. Soc. 114 (1992) 7581.

[11] G.E. Jones, D.A. Kendrick, A.B. Holmes, Org. Synth. Coll. 8 (1993) 63.

[12] S.R. Hall, H.D. Flack, J.M. Stewart (Eds.),The XTAL 3.2 Users Manual, Universities of Western Australia, Geneva and Maryland, 1992.